Bridging the Gap between the Gas and Solution Phase: Solvent Specific Photochemistry in 4-*tert*-Butylcatechol

Michael D. Horbury, Lewis A. Baker, Wen-Dong Quan, Jamie D. Young, Michael Staniforth, Simon E. Greenough, and Vasilios G. Stavros*

Department of Chemistry, University of Warwick, Gibbet Hill Road, Coventry, CV4 7AL, UK.

ABSTRACT: Eumelanin is a naturally synthesized ultraviolet light absorbing biomolecule, possessing both photoprotective and phototoxic properties. We infer insight into these properties of eumelanin using a bottom-up approach, by investigating a subunit analogue, 4-*tert*-butylcatechol. Utilizing a combination of femtosecond transient electronic absorption spectroscopy and time-resolved velocity map ion imaging, our results suggest an environmental-dependent relaxation pathway, following irradiation at 267 nm to populate the S_1 ($^1\pi\pi^*$) state. Gas-phase and non-polar solution-phase measurements reveal that the S_1 state decays through coupling onto the S_2 ($^1\pi\sigma^*$) state that is dissociative along the non-intramolecular hydrogen bonded 'free' O–H bond. This process is mediated by tunneling beneath an S_1/S_2 conical intersection and occurs in 4.9 ± 0.6 ps in the gas-phase and 27 ± 7 ps in the non-polar cyclohexane solution. Comparative studies on the deuterated isotopologue of 4-*tert*-butylcatechol in both the gas- and solution-phase (cyclohexane) reveals an average kinetic isotope effect of ~19 and ~7, respectively, supportive of O–H dissociation mediated by a quantum tunneling mechanism. In contrast, in the polar acetonitrile, the S_1 state decays on a much longer timescale of 1.7 ± 0.1 ns. We propose that the S_1 decay is now multicomponent, likely driven by internal conversion, intersystem crossing and fluorescence, as well as O–H dissociation. The attribution of conformer driven excited state dynamics to explain how the S_1 state decays in the gas- and non-polar solution-phase *versus* the polar solution-phase, elegantly demonstrates the influence the environment has on the ensuing excited state dynamics.

1. INTRODUCTION

The photoexcited state dynamics of biomolecules have borne extensive interest in the field of photochemistry due, in part, to an apparent relative photostability present in key biochemical systems, despite the fact that they contain ultraviolet (UV) chromophores.[1-4] The absorption of UV radiation has the ability to cause bond dissociation within molecules, which can lead to undesired chemical changes; mutagenesis in DNA being a prime example.[5] In order for biomolecules to be photostable after UV absorption, they must be able to efficiently redistribute any excess energy away from such harmful pathways. Typically, these non-dissociative processes must occur on an ultrafast (femtosecond (fs) to picosecond (ps)) timescale in order to kinetically out-compete the destructive pathways; however, notable exceptions of longer-lived excited states do exist, *e.g.* DNA excimers.[6]

Employing a *bottom-up* approach, in which the UV chromophore subunit of a larger biomolecule is isolated and studied,[2,3] can lend valuable insights from which we may begin to understand the photochemistry of the larger biomolecule as a whole. Much of the previous work in this field has been performed in the isolated gas-phase,[2-3,7-13] which proves successful in recovering information about the molecular dynamics of these UV chromophores without the presence of environmental effects. Whilst this provides a good starting point for the interpretation of excited state dynamics in larger systems, interactions with surrounding solvent and solute molecules need to be taken into consideration in order to develop a more complete picture of photostability in nature.[14] Placing a chromophore in solution allows for environmental perturbations on the chromophore to be studied, more closely matching the native environment of such biomolecules. A comparison of gas- and solution-phase dynamics has been previously performed on an amino acid subunit, the UV chromophore phenol.[15,16] Subtle differences between the two phases were observed, supporting the postulate that the local environment of biomolecules can play an important role in the molecule's photodynamics, whilst also highlighting that knowledge of the dynamics in the gas-phase is highly transferable and complementary to solution-phase studies.

Many other phenol analogues have also been studied in the gas-phase,[17-21] one of which is catechol (1,2-dihydroxybenzene) - a UV chromophore in a range of biomolecules, one of which is eumelanin. As one of three types of melanin,[22] eumelanin is largely responsible for skin's frontline defense to UV exposure.[23-24] However, gaining a complete understanding of its photodynamics is ongoing, with much progress to be made,[25-28] evidenced by recent work implicating the long-term (after many hours of UVA exposure) phototoxicity of eumelanins.[29] Previous gas-phase studies of catechol[21] have shown that after excitation to the first excited $^1\pi\pi^*$ state (S_1), H-atom elimination is observed from dissociation of the non-intramolecular hydrogen bonded 'free' O–H bond, leading to the formation of the catechoxyl radical in approximately 10 ps. Immediately, this suggests that catechol is not photostable following UV exposure, and yet it is a subunit of a photoprotective biomolecule.[26] In nature, eumelanin resides within an organelle as large hetero-polymer fibrils,[30] thus gas-phase studies are unable to fully capture the photodynamics of catechol in this native environment. Therefore, we ask: do the natural surroundings of catechol influence its photodynamics?

In the present study, we try to address this question. Owing to catechol's poor solubility in non-polar solvents, the functionalized catechol, 4-*tert*-butylcatechol (termed 4-TBC hereon), is

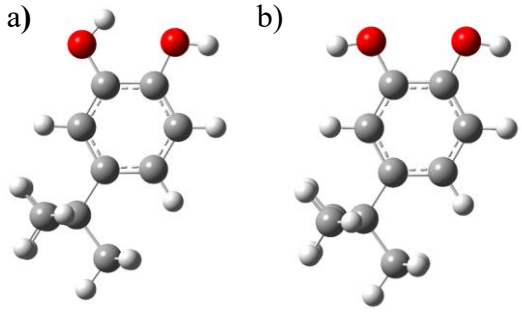

Figure 1. 'Gas-phase' calculations of the first a) and second b) lowest energy conformers ('closed' and 'open' respectively) in the ground electronic (S_0) state of 4-TBC. Molecular geometries calculated in Gaussian 09a using the M052X functional with a 6-311G** basis set. See SI for details.

used instead, shown in Figure 1. In order to gauge how well 4-TBC performs as a proxy for catechol, we performed gas-phase time-resolved velocity map ion imaging (TR-VMI) and time-resolved ion yield (TR-IY) measurements. To model the role that the surrounding solvent plays in the excited state dynamics of 4-TBC after excitation to the S_1 state, we employ fs transient electronic (UV-visible) absorption spectroscopy (TEAS), using the weakly perturbing, non-polar solvent, cyclohexane, and the highly perturbing polar solvent, acetonitrile.

II. METHODS

The detailed experimental procedures pertaining to TR-VMI, TR-IY and TEAS have been extensively described elsewhere.[31-33] Briefly, a commercially available Ti:Sapphire oscillator and amplifier system (Spectra-Physics) produces 3 mJ laser pulses of ~40 fs duration centred at 800 nm and a repetition rate of 1 kHz. For TR-VMI and TR-IY two optical parametric amplifiers (Light Conversion TOPAS-C), each pumped with ~1 mJ/pulse at 800 nm, produce tunable UV pump and probe pulses ($h\nu_{pu}$ and $h\nu_{pr}$ respectively). $h\nu_{pu}$ is centred at 267 nm (~6 μJ/pulse) and is temporally varied with respect to the probe using a hollow gold retroreflector mounted on a motorized stage, which enables a maximum temporal delay of Δt = 1.2 ns to be achieved. $h\nu_{pr}$ is set to 243 nm (~7 μJ/pulse) to resonantly ionize H-atoms. Both beams are then focused, near-collinearly, into the VMI spectrometer, perpendicularly intersecting a molecular beam of 4-TBC (95%, Sigma-Aldrich) seeded in 2 bar of helium. The molecular beam is formed by supersonic jet expansion from an Even-Lavie pulsed solenoid valve[34] heated to 100 ^{o}C, and is passed through a 2 mm conical skimmer. The VMI spectrometer is in line with the molecular beam and follows the standard Eppink and Parker design.[35] After photolysis of 4-TBC with $h\nu_{pu}$, resulting H-atoms are ionized with $h\nu_{pr}$. The VMI optics project the 3-D velocity distribution of H^+ ions towards a position sensitive detector which consists of a pair of micro-channel plates and a P-43 phosphor screen (Photek, VID-240), the emitted light being captured on a CCD camera (Basler, A-312f). The original 3-D velocity distribution is reconstructed from the resulting 2-D image using an image reconstruction algorithm.[36] Radial pixels on the image are converted into total kinetic energy release (TKER) using the appropriate Jacobian, calibration factor and co-fragment mass, generating the desired 1-D TKER spectra. For TR-IY, we simply record the appearance of the parent ion signal (4-TBC$^+$) as a function of Δt, by gating the detector on this signal and recording the total emitted light registered on the detector.

For TEAS, a 1 mJ/pulse 800 nm laser beam is split into two beams of: (i) 0.95 mJ/pulse and (ii) 0.05 mJ/pulse. (i) is used to generate $h\nu_{pu}$ centred at 267 nm (1–2 mJcm^{-2}) through second and then third harmonic generation using two beta-barium borate crystals. (ii) is used to generate $h\nu_{pr}$, a white light continuum (330-675 nm). Pump-probe polarizations are held at magic angle (54.7°) relative to one another. Changes in optical density (ΔOD) of the sample were calculated from probe intensities, collected using a spectrometer (Avantes, AvaSpec-ULS1650F). The delivery system for the samples (4-TBC in either cyclohexane (100%, VWR) or acetonitrile (99.9%, VWR)) is a flow-through cell (Demountable Liquid Cell by Harrick Scientific Products, Inc.). The sample is circulated using a PTFE tubing peristaltic pump (Masterflex) recirculating sample from a 50 ml reservoir in order to provide each pump-probe pulse-pair with fresh sample.

Comparative TR-VMI and TEAS studies also were carried out on the deuterated isotopologue of 4-TBC, *i.e.*, 4-TBC-d_2, in which we have selectively deuterated both O–H bonds ($C_{10}H_{12}O_2D_2$) synthesized and characterized according to the description provided in the supporting information (SI). For the TEAS, a bespoke sample delivery system was implemented in order to keep the sample in a dry, inert atmosphere to minimize isotopic exchange. Further details are provided in the SI.

III. RESULTS and DISCUSSION

a. Gas-phase studies

Figure 2a shows an example TKER spectrum with the image from which it was extracted shown inset; the left side corresponds to the recorded H^+ image while the right half shows the reconstructed slice through the centre of the 3-D ion distribution (the black arrow indicates the electric field polarization, $\boldsymbol{\varepsilon}$, of the pump pulse). A pump wavelength of 267 nm (4.65 eV) was used to photoexcite 4-TBC to the S_1 state, with the generated H-atoms, associated with O–H dissociation, subsequently ionized *via* a [2+1] resonance enhanced multiphoton ionization (REMPI) scheme. The pump-probe time delay (Δt) used when recording this particular image was set at Δt = 1.2 ns. A high kinetic energy (KE) feature is apparent in the TKER spectrum centered at ~7000 cm^{-1}, which returns to the baseline by ~10,000 cm^{-1}. This high-KE signature strongly accords with our previous work in catechol,[21] and is associated with H-atoms generated through dissociation of the 'free' (non-hydrogen bonded) O–H bond (see Figure 1a) to yield the 4-*tert*-butylcatecoxyl radical $C_{10}H_{13}O_2(X)$ (termed 4-TBC$^{\bullet}$ hereon) plus H photoproduct, *via* the dissociative (O–H coordinate) $^1\pi\sigma^*$ surface (S_2).

Collecting a series of TKER spectra at varying Δt and then integrating the high KE feature over the range ~5500-8500 cm^{-1} results in the H^+ transient shown in Figure 2b (blue circles). In order to obtain a time constant for the S_2 mediated O–H dissociation, a kinetic fit to the data is applied, comprising two exponential rise functions convoluted with our instrument response (~120 fs full width half maximum), shown by the blue line. Two (gas-phase, *g*) time constants (τ) are returned: $^g\tau_{MP}$ >30 fs, which is associated with multiphoton processes (MP),[37-

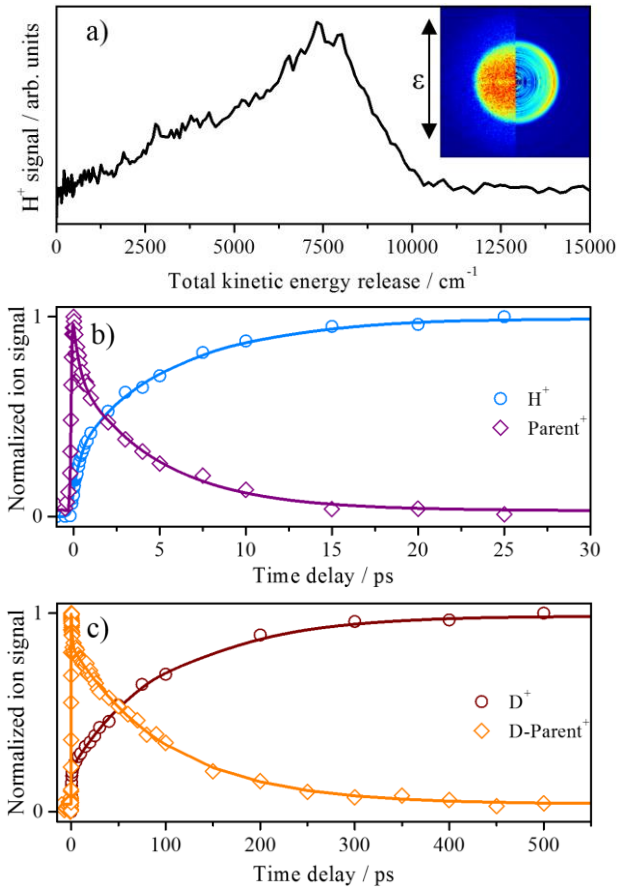

Figure 2. a) TKER spectrum of TBC following excitation at 267 nm and probing H-atom photoproducts with a 243 nm probe pulse at Δt = 1.2 ns. Inset: H^+ velocity map image, left half showing raw image, right half showing reconstructed image. b) Normalized integrated H^+ signal transient (blue circles) and the corresponding parent ion signal transient (purple diamonds), solid lines show the kinetic fits. c) Normalized integrated D^+ signal transient (dark brown circles) and the corresponding parent (4-TBC-d_2^+) ion signal transient (light brown diamonds). Solid lines show kinetic fit.

[38] and a slower rise in the H^+ (and thus H-atom) signal, ${}^g\tau_{H^+} = 5.9 \pm 0.3$ ps, which we attribute to quantum tunneling beneath an S_1/S_2 conical intersection (CI, *vide infra*).[21] In addition to the H^+ transient, Figure 2b also shows a complementary TR-IY trace of the 4-TBC$^+$ parent ion signal, as a function of Δt (purple diamonds), which provides a measure of the dynamics occurring on the photoprepared S_1 state following excitation at 267 nm. Cursory inspection of the 4-TBC$^+$ parent transient relative to the corresponding H^+ transient reveals that the S_1 state decays on a similar timescale to the appearance of H-atoms associated with O–H dissociation. Indeed, fitting this transient with a bi-exponential decay function (purple line) returns time constants of ${}^g\tau_{IVR(H)} = 0.4 \pm 0.1$ ps, associated with rapid intramolecular vibrational energy redistribution (IVR) in the S_1 state as seen in our previous investigation,[21] and ${}^g\tau_{P^+} = 4.9 \pm 0.6$ ps, which is assigned to excited state population flux from the S_1 state, the P^+ signifying decay of the non-deuterated isotopologue parent ion signal (and therefore S_1 state population). Importantly, this shows a clear correlation to the appearance time of H^+.

To confirm the role of tunneling following photoexcitation to S_1, we have also carried out measurements on 4-TBC-d_2. The results of both the D^+ and 4-TBC-d_2^+ transients are shown in Figure 2c. Kinetic fits to the transients return time-constants of ${}^g\tau_{D^+} = 98 \pm 2$ ps and ${}^g\tau_{DP^+} = 102 \pm 3$ ps and thus an average kinetic isotope effect (KIE, k_H/k_D) of ~19. Here the time-constant typography has the same meaning as above, but applied to the deuterated isotopologue. The large KIE obtained here is a telltale signifier that the 'free' O–H dissociation is very likely mediated through tunneling under the S_1/S_2 CI. For completeness, we also note that ${}^g\tau_{IVR(D)} = 1.0 \pm 0.1$ ps compares favorably with the value extracted for the non-deuterated isotopologue. Notably, the KIE obtained for 4-TBC accords well with similar measurements carried out in catechol, which returned a KIE ~30, validating the use of 4-TBC as a proxy for catechol (*vide supra*).

b. Solution-phase studies

The non-polar solvent, cyclohexane, was used as the starting point for unraveling the solution-phase dynamics of 4-TBC, as the weakly perturbing environment of cyclohexane serves as a good model for the gas-phase environment. Figure 3a shows transient absorption spectra (TAS) of 4-TBC in cyclohexane, following 267 nm (4.65 eV) excitation, having two main features at early Δt (~1-5 ps); a peak centered around 370 nm and another broader feature centered at 495 nm. These features are attributed to the excited state absorption (ESA) from the S_1 state to higher-lying S_n states.[15,32] At Δt = 5 ps, peaks at 375 and 390 nm appear to lie on top of the S_1 absorption; these peaks are the signature absorption of 4-TBC$^\bullet$ in concordance with literature on other phenols.[39,40] The peak at 390 nm (and to a lesser extent 375 nm) appears to narrow as the spectra evolve over time (Δt = 5-40 ps). This may be explained by quenching of the initially produced hot radical through vibrational energy transfer (VET).[41,42] Figure 3b (red circles) shows a transient acquired by integrating a 5 nm wide slice of the TAS, centered on 450 nm, as a function of Δt. This wavelength is chosen due to the absence of radical absorption in this region, ensuring that signal at this wavelength will come primarily from S_1 absorption. This transient was fit with a tetra-exponential decay function (red line); the first three exponentials account for the cyclohexane solvent response alone (see SI for further details). The single time constant found for (non-deuterated i.e. H) 4-TBC in cyclohexane (*c*), ${}^c\tau_{(H)} = 27 \pm 7$ ps, is assigned to excited state population flux out of the S_1. TAS of 4-TBC-d_2 (see SI for details) were also recorded to acquire a corresponding 4-TBC-d_2 transient centered at 450 nm (again using a 5 nm integration around this spectral region) (Figure 3b, blue diamonds). Our kinetic fit (blue line) returns an S_1 lifetime for the deuterated (D) species of ${}^c\tau_{(D)} = 190 \pm 20$ ps and thus a KIE of ~7. Whilst the KIE returned from the cyclohexane measurements is less than that obtained from the gas-phase measurements (*cf.* KIE ~19), this still suggests O–H dissociation likely occurs along a pathway that is mediated by tunneling through a potential barrier.[43]

We now begin to evaluate the environmental influence on the excited state dynamics of 4-TBC by using a more perturbative, polar solvent. Acetonitrile was selected due to its high polarity and (apparent) low reactivity towards 4-TBC. Figure 3c shows the TAS of 4-TBC in acetonitrile. The main feature at early Δt is a broad ESA across the entire probe window, which we once again attribute to absorption from the S_1 state to higher-

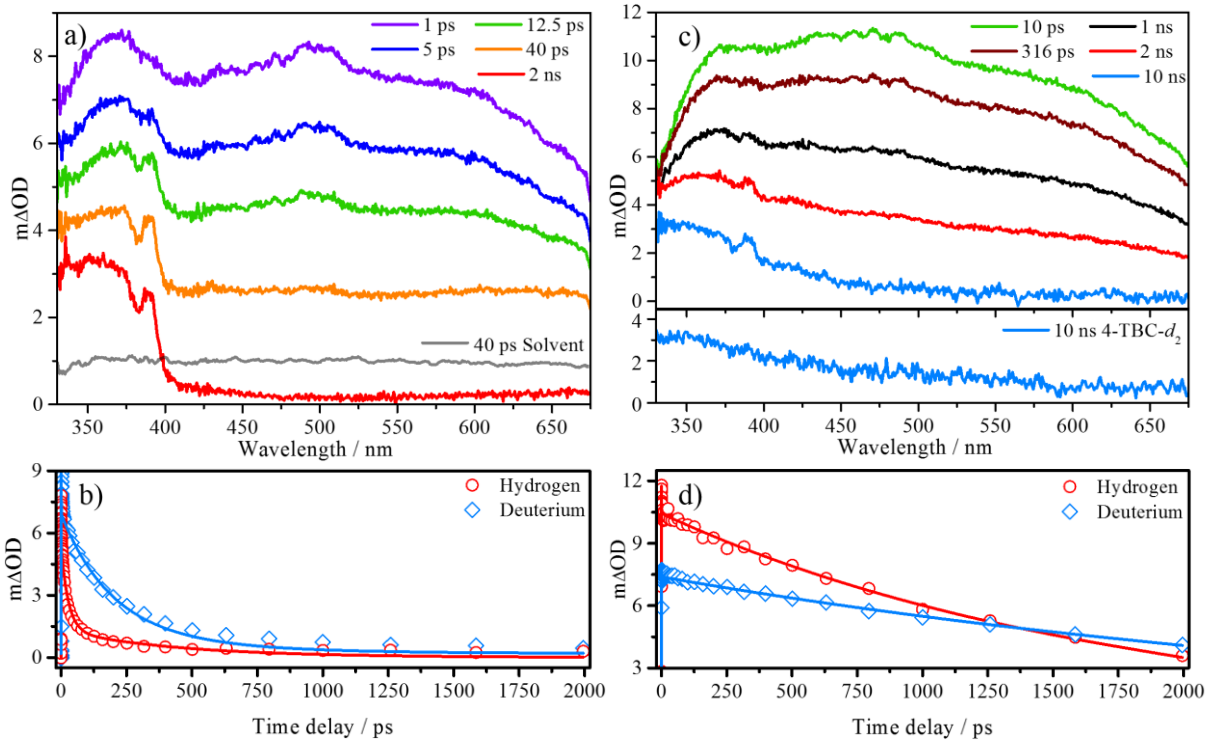

Figure 3. a) Selection of TAS of 35 mM 4-TBC in cyclohexane with an excitation wavelength of 267 nm. b) Transient slices of 35 mM 4-TBC in cyclohexane (red circles) and 35 mM 4-TBC-d_2 in cyclohexane (blue diamonds) acquired by integrating over a 5 nm window centered at 450 nm; solid lines are the kinetic fits. c) Selection of TAS of 35 nm mM 4-TBC in acetonitrile and 30 mM 4-TBC-d_2 in acetonitrile (bottom trace) with an excitation wavelength of 267 nm. d) Transient slices of 35 mM 4-TBC in acetonitrile (red circles) and 30 mM 4-TBC-d_2 in acetonitrile (blue diamonds) acquired by integrating over a 5 nm centered at 450 nm; solid lines are the kinetic fits. Note that optical density is plotted in the range mΔOD = 3-12 to magnify the extended decay.

lying S_n states.[15,32] At Δt = 300 ps, a smaller peak, which is assigned to the 4-TBC$^{\bullet}$ absorption, sits atop the S_1 state absorption at 390 nm. Beyond Δt = 2 ns, this radical signature appears more defined and the S_1 state absorption has decayed away sufficiently to reveal an absorption resembling that of an excited triplet state.[44] By Δt = 10 ns the S_1 absorption has completely decayed yielding the triplet state and radical species absorptions, reminiscent of previous studies in guaiacol.[32] TAS of 4-TBC-d_2 in acetonitrile do not show (within the signal-to-noise) the radical absorption; a Δt = 10 ns TAS is shown in the lower panel in Figure 3c to highlight this (see discussion below). Unlike the transients obtained in cyclohexane, the transient in acetonitrile (Figure 3d) requires only two exponential decay functions to fit the data (red line), both of which are attributed to solute-only dynamics. Solvent contribution from acetonitrile was negligible (see SI for details). The (acetonitrile, *a*) time-constants returned from the kinetic fit are ${}^{a}\tau_{IVR(H)}$ = 230 ± 50 fs and ${}^{a}\tau_{(H)}$ = 1.7 ± 0.1 ns. The very fast decay manifests due to a decrease in the excited state absorption as the Franck-Condon overlap for the S_n ¬ S_1 absorption evolves due to IVR, evidently resulting in a reduction of the overlap between the S_1 and S_n states. Whilst these dynamical processes are intriguing, we are unable to resolve a similar decay pathway in 4-TBC/cyclohexane, due to the very large solvent-only dynamics at short time-delays, and they do not contribute to the main focus of this current work, so they are not discussed further.

The second extracted time-constant, ${}^{a}\tau_{(H)}$ = 1.7 ± 0.1 ns, is assigned to excited state population flux out of the S_1 state in concord with our previous studies on guaiacol.[32] Intriguingly, we note there is a >50-fold increase in the lifetime of the S_1 state in acetonitrile relative to cyclohexane (*cf.* ${}^{c}\tau_{(H)}$ = 27 ± 7 ps), the significance of which is discussed below. TAS of 4-TBC-d_2 in acetonitrile collected and then integrated with a 5 nm wide slice centered around 450 nm yielded a similar transient (Figure 3d). Our kinetic fit (blue line) returned an S_1 lifetime of ${}^{a}\tau_{(D)}$ = 3.3 ± 0.1 ns (as well as ${}^{a}\tau_{IVR(D)}$ = 180 ± 50 fs for completeness) and thus a KIE of ~1.9.

c. The gas- *versus* solution-phase studies

We now compare our findings between the gas- and solution-phase. In the gas-phase, the parent^{+} transient, which directly reports on the S_1 lifetime, returns a time-constant of ${}^{g}\tau_{(H)}$ = 4.9 ± 0.6 ps whilst the S_1 lifetime in cyclohexane is ${}^{c}\tau_{(H)}$ = 27 ± 7 ps. The almost six-fold increase in the S_1 lifetime in cyclohexane may be attributed to the very modest polarity of cyclohexane (dielectric constant (ε_r) = 2.02), which will perturb, albeit weakly, the electronic state energies. The KIE returned from both the gas- and solution-phase (gas ~19, solution ~7) strongly suggests that, following excitation to S_1, O–H dissociation proceeds along a barriered pathway. Our attribution of tunneling mediated dissociation along the 'free' O–H bond, beneath an S_1/S_2 CI, also accords with previous studies on phenols in the gas- and solution-phase (see reference 2 and references therein). Studies on substituted phenols have also shown the quite dramatic effect substituents have on the topography of either the S_1 or S_2 (or both) potential energy surface (PES), resulting in noticeable effects on the S_1/S_2 tunneling probability and

hence S_1 lifetime.[17-18,21,45,46] Similar effects on the local topography of the S_1 or S_2 PESs from a weakly perturbing solvent will undoubtedly have a similar effect on the S_1 lifetime as observed here.

Whilst the gas-phase studies compare favorably with those in the non-polar cyclohexane, as expected, this is not the case in acetonitrile (ε_r = 37.5). The S_1 lifetime, ${}^{a}\tau_{(H)}$ = 1.74 ± 0.1 ns, is >50 times that of 4-TBC in cyclohexane and >350 times that of gas-phase 4-TBC (${}^{c}\tau_{(H)}$ = 27 ± 7 ps and ${}^{g}\tau_{(H)}$ = 4.9 ± 0.6 ps respectively). The polar acetonitrile is thought to induce the same conformer change to 4-TBC as with catechol, where the intramolecular hydrogen bond is broken, resulting in two intermolecular hydrogen bonds with the solvent.[27,36] To explore the role of conformational change on the observed dynamics, time-dependent density functional theory calculations were performed with the Gaussian09[47] package using both the M052X[48] and CAM-B3LYP[49] functionals and a 6-311G**[50] basis set. These calculations show that the 'open' and 'closed' conformers are planar in the S_0 state (see Figure 1 and SI). In contrast, in the S_1 state, whilst the 'open' conformer retains planarity, the 'closed' conformer becomes distorted (see SI).

In the gas-phase and in cyclohexane, the photoexcited S_1 state is non-planar. The non-planar 'closed' conformer has been proposed to explain the dramatic decrease in S_1 lifetime in catechol relative to phenol (due to symmetry enhanced tunneling).[20,21] A similar reasoning can be applied here for 4-TBC in both non-perturbing environments. In the polar solvent acetonitrile, the photoexcited S_1 state likely retains a planar 'open' geometry. Such a conformer change (with solvent polarity) has also been observed in guaiacol,[51,52] resulting in considerably altered photodynamics.[32] In 4-TBC we see an analogous alteration in the observed photodynamics of the S_1 excited state in the form of an increased lifetime, an appearance of the triplet state absorption at large values of Δt and a smaller radical absorption

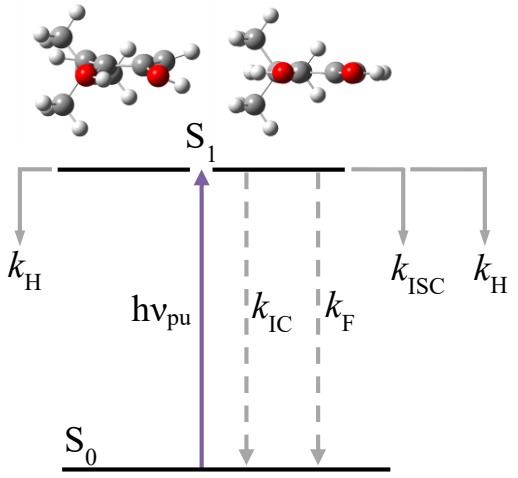

Figure 4. Schematic representation of the observed decay processes in 4-TBC. The left panel demonstrates the S_1 decay of the 'closed' (non-planar) conformer, which dominates in the gas-phase and in the non-polar cyclohexane. The right panel shows the S_1 decay of the 'open' (planar) conformer, which dominates in the polar acetonitrile. Dashed grey arrows represent processes that our current measurements cannot probe and are based on previous work in phenol.[15]

appearing at Δt ~300 ps and beyond; dynamics which are extremely similar to those seen for guaiacol in methanol[32] as well as bearing resemblance to their archetype, phenol in cyclohexane.[15,16] This leads to the conclusion that a solvent-induced conformer change causes the suppression of the O–H bond fission pathway (likely due to an enhanced barrier to tunneling) allowing for additional decay pathways such as internal conversion (IC), fluorescence and intersystem crossing (ISC) to effectively compete with 'free' O–H dissociation.[15,32,53] The absence of 4-TBC-$d_2^{\bullet}$ out to Δt = 10 ns in our deuterated studies supports this idea; O–D bond fission is kinetically outcompeted by other pathways, which is unsurprising given that D-atom tunneling through the barrier beneath an S_1/S_2 CI will be significantly suppressed. As such, we see an increase in the triplet state signal.

On the basis of our discussion above, a proposed schematic summarizing the various decay pathways in 4-TBC, both in perturbative and non-perturbative environments, is given in Figure 4. Photoexcitation with 267 nm radiation, prepares 4-TBC in the S_1 state. In the gas-phase, the excited state decays through dissociation of the 'free' O–H bond, along a pathway that has a barrier. The KIE of ~19 strongly suggests that O–H dissociation is mediated through tunneling beneath the S_1/S_2 CI. In the weakly perturbing cyclohexane solvent, the photoexcited S_1 state decay appears to follow a similar path: tunneling mediated O–H dissociation. While a milder KIE ~7 makes this supposition less conclusive, it is still strongly supportive of a barriered O–H dissociation coordinate. The left side of Figure 4 contains a single, dominant process involved in the non-perturbative, gas-phase and weakly perturbative, (cyclohexane) solution-phase: k_H signifies the rate constant of O–H dissociation. In the strongly perturbing acetonitrile solvent, we have contrasting dynamics. The 'open' conformer, which now dominates, displays a diminished 4-TBC$^{\bullet}$ feature. Upon deuteration, the 4-TBC-$d_2^{\bullet}$ absorption signature is almost completely extinguished. Instead, the excited state decay reveals an absorption feature in the TAS that is reminiscent of triplet state absorption. As a consequence, we propose that excited state decay in 4-TBC (acetonitrile) is multicomponent, including O–H dissociation, ISC and likely IC and fluorescence, characterized by associated rate constants k_H, k_{ISC}, k_{IC} and k_F respectively. The right side of Figure 4 shows this process.

We close by returning to the original question regarding whether the natural surroundings impact the photostability of biomolecules. In 4-TBC, a close analogue to the catechol chromophore, it is clear that the photoinduced dynamics in non-perturbing environments compare favorably with those in the gas-phase; both cases involve O–H dissociation to yield the phototoxic radical species 4-TBC$^{\bullet}$.[54] When 4-TBC is placed into a polar solvent, this pathway is severely suppressed. This is a consequence of a change in molecular geometry through solvent interactions. This structural change reduces the excited state decay, with the phototoxic radical pathway becoming less favorable, and opens up alternative (and competitive) relaxation pathways, including potentially harmful triplet state formation.[29] Interestingly, the triplet state formation accords with previous studies by Sundström and coworkers on 5,6-dihydroxyindole,[28] one of the main building blocks of eumelanin, which incorporates the catechol chromophore. Thus, the present bottom-up study provides a key steppingstone between a model UV chromophore in the gas phase and a larger biomolecule within its

native environment. This emphasizes the critical role of environment-induced photodynamics.

IV. CONCLUSIONS

The excited state dynamics of 4-TBC have been investigated in both gas- and solution-phase using a combination of TR-VMI, TR-IY and TEAS, following photoexcitation of the S_1 ($^1\pi\pi^*$) state at 267 nm. Through the recorded gas-phase TKER spectra and associated H^+ transient, a time constant for H-atom elimination of ${}^g\tau_{H^+} = 5.9 \pm 0.3$ ps is found. Complementary TR-IY of the parent$^+$ transient yields a time constant of ${}^g\tau_{P^+} = 4.9 \pm 0.6$ ps. Comparative studies in 4-TBC-d_2 yield time constants of ${}^g\tau_{D^+} = 98 \pm 2$ ps and ${}^g\tau_{DP^+} = 102 \pm 3$ ps and thus an average KIE of ~19. A dominant dissociation of the non-intramolecular hydrogen bonded 'free' O–H bond is deduced, very likely mediated through tunneling beneath an S_1/S_2 CI. Solution-phase studies in the weakly perturbing cyclohexane solvent yield excited state decay time constants of ${}^c\tau_{(H)} = 27 \pm 7$ ps and ${}^c\tau_{(D)} = 190 \pm 20$ ps for 4-TBC and 4-TBC-d_2 respectively. The KIE of ~7 implies, together with the emergent 4-TBC-$d_2^\bullet$ feature, that a similar relaxation pathway in 4-TBC/cyclohexane is operative as in 4-TBC in the gas-phase. In the strongly perturbing, polar acetonitrile solvent, excited state decay occurs with time constants of ${}^a\tau_{(H)} = 1.7 \pm 0.1$ ns and ${}^a\tau_{(D)} = 3.3 \pm 0.1$ ns for 4-TBC and 4-TBC-d_2 respectively. The dominant decay channel in acetonitrile is no longer O–H dissociation, but rather multicomponent, involving ISC, IC and fluorescence together with O–H dissociation. The dramatic differences in excited state lifetime in the two solvents, is attributed to conformational change between 4-TBC (and 4-TBC-d_2) in cyclohexane and acetonitrile, in which, respectively, the closed and open conformers dominate. This result thus serves to highlight the critical importance of the influence of structure on dynamics.

ASSOCIATED CONTENT

Supporting Information

Static absorption spectra, additional experimental details, fitting procedures for presented transients, deuterated TAS, solvent-only transients and further computational details.

AUTHOR INFORMATION

Corresponding Author

v.stavros@warwick.ac.uk

Notes

The authors declare no competing financial interest.

ACKNOWLEDGMENTS

The authors are grateful to Ms Faye Monk, Mr Connor Gallagher and Mr Peter Brindley for experimental assistance and Dr Gareth Roberts (University of Bristol) for helpful discussions. M.D.H. and J.D.Y. thank the University of Warwick for EPSRC doctoral training awards. L.A.B., W.D.Q. thank the EPSRC for providing studentships under grant number EP/F500378/1, through the Molecular Organisation and Assembly in Cells Doctoral Training Centre. M.S. and S.E.G thank the EPSRC and the Warwick Institute of Advanced Studies, respectively, for postdoctoral funding. M.S. also thanks Prof. Martin Paterson (Heriot Watt) for use of his computational facilities. V.G.S. thanks the EPSRC for an equipment grant (EP/J007153) and the Royal Society for a University Research Fellowship.

REFERENCES

(1) Sobolewski, A.; Domcke, W. Molecular Mechanisms of the Photostaility of Life. *Phys. Chem. Chem. Phys.* **2010**, *12*, 4897-4898.

(2) Roberts, G. M.; Stavros, V. G. The Role of πσ* States in the Photochemistry of Heteroaromatic biomolecules and their subunits: insights from gas-phase femtosecond spectroscopy. *Chem. Sci.* **2014**, *5*, 1698-1722.

(3) Staniforth, M.; Stavros, V. G. Recent advances in experimental techniques to probe fast excited-state dynamics in Biological Molecules in the Gas Phase: Dynamics in Nucleotides, Amino Acids and Beyond. *Proc. R. Soc. A.* **2013**, *469* 20130458.

(4) Crespo-Hernández, C. E.; Cohen, B.; Hare, P. M.; Kohler, B. Ultrafast Excited-State Dynamics in Nuleic Acids. *Chem. Rev.* **2004**, *104*, 1977-2019.

(5) Pfeifer, G. P.; You, Y.-H.; Besaratinia, A. Mutations Induced by Ultraviolet Light. *Mutat. Res.* **2005**, *571*, 19-31.

(6) Middleton, C. T.; de La Harpe, K.; Su, C.; Law, Y. K.; Crespo-Hernández, C. E.; Kohler, B. DNA Excited-State Dynamics: From Single Bases to the Double Helix. *Annu. Rev. Phys. Chem.* **2009**, *60*, 217-239.

(7) de Vries, M. S.; Hobza, P. Gas-phase Spectroscopy of Biomolecular Building Blocks. *Annu. Rev. Phys. Chem.* **2007**, *58*, 585-612.

(8) Ashfold, M. N. R.; Cronin, B.; Devine, A. L.; Dixon, R. N.; Nix, M. G. D. The Role of πσ* Excited
States in the Photodissociation of Heteroaromatic Molecules. *Science* **2006**, *312*, 1637-1640.

(9) Ullrich, S.; Schultz, T.; Zgierski, M. Z.; Stolow, A. Electronic Relaxation Dynamics in DNA and RNA Bases Studied by Time-Resolved Photoelectron Spectroscopy. *Phys. Chem. Chem. Phys.* **2004**, *6*, 2796-2801.

(10) Nix, M. G. D.; Devine, A. L.; Cronin, B.; Ashfold, M. N. R. Ultraviolet Photolysis of Adenine: Dissociation via the $^1\pi\sigma^*$ State. *J. Chem. Phys.* **2007**, *126*, 124312.

(11) Wells, K. L.; Hadden, D. J.; Nix, M. G. D.; Stavros, V. G. Competing πσ* States in the Photodissociation of Adenine. *J. Phys. Chem. Lett.* **2010**, *1*, 993-996.

(12) Iqbal, A.; Stavros, V. G. Active Participation of $^1\pi\sigma^*$ States in the Photodissociation of Tyrosine and its Subunits. *J. Phys. Chem. Lett.* **2010**, *1*, 2274-2278.

(13) Evans, N. L.; Ullrich, S. Wavelength Dependence of Electronic Relaxation in Isolated Adenine Using UV Femtosecond Time-Resolved Photoelectron Spectroscopy. *J. Phys. Chem. A* **2010**, *114*, 11225-11230.

(14) Elles, C. G.; Crim, F. F. Connecting Chemical Dynamics in Gases and Liquids. *Annu. Rev. Phys. Chem.* **2006**, *57*, 273-302.

(15) Zhang, Y.; Oliver, T. A. A.; Ashfold, M. N. R.; Bradforth, S. E. Contrasting the Excited State Reaction Pathways of Phenol and Para-methylthiophenol in the Gas and Liquid Phases. *Faraday Discuss.* **2012**, *157*, 141-163.

(16) Harris, S. J.; Murdock, D.; Zhang, Y.; Oliver, T. A.; Grubb, M. P.; Orr-Ewing, A. J.; Greetham, G. M.; Clark, I. P.; Towrie, M.; Bradforth, S. E.; Ashfold, M. N. R. Comparing Molecular Photofragmentation Dynamics in the Gas and Liquid Phases. *Phys. Chem. Chem. Phys.* **2013**, *15*, 6567-6582.

(17) Hadden, D. J.; Roberts, G. M.; Karsili, T. N. V.; Ashfold, M. N. R.; Stavros, V. G. Competing $^1\pi\sigma^*$ Mediated Dynamics in Mequinol: O–H *versus* O–CH_3 Photodissociation Pathways. *Phys. Chem. Chem. Phys.* **2012**, *14*, 13415-13428.
(18) Young, J. D.; Staniforth, M.; Chatterley, A. S.; Paterson, M. J.; Roberts, G. M.; Stavros, V. G. Relaxation Dynamics of Photoexcited Resorcinol: Internal Conversion *versus* H Atom Tunnelling. *Phys. Chem. Chem. Phys.* **2013**, *16*, 550-562.
(19) Livingstone, R. A.; Thompson, J. O. F.; Iljina, M.; Donaldson, R. J.; Sussman, B. J.; Paterson, M. J.; Townsend, D. Time-Resolved Photoelectron Imaging of Excited State Relaxation Dynamics in Phenol, Catechol, Resorcinol, and Hydroquinone. *J. Phys. Chem.* **2012**, *137*, 184304.
(20) Weiler, M.; Miyazaki, M.; Féraud, G.; Ishiuchi, S.-i.; Dedonder, C.; Jouvet, C.; Fujii, M. Unusual Behavior in the First Excited State Lifetime of Catechol. *J. Phys. Chem. Lett.* **2013**, *4*, 3819-3823.
(21) Chatterley, A. S.; Young, J. D.; Townsend, D.; Zurek, J. M.; Paterson, M. J.; Roberts, G. M.; Stavros, V. G. Manipulating Dynamics with Chemical Structure: Probing Vibrationally-Enhanced Tunnelling in Photoexcited Catechol. *Phys. Chem. Chem. Phys.* **2013**, *15*, 6879-92.
(22) Meredith, P.; Sarna, T. The Physical and Chemical Properties of Eumelanin. *Pigm. Cell Res.* **2006**, *19*, 572-594.
(23) Kollias, N.; Sayre, R. M.; Zeise, L.; Chedekel, M. R. New Trends in Photobiology: Photoprotection by Melanin. *J. Photochem. Photobiol. B: Biol.* **1991**, *9*, 135-160.
(24) Sarna, T. New trends in photobiology: Properties and function of the ocular melanin a photobiophysical view. *J. Photochem. Photobiol. B: Biol.* **1992**, *12*, 215-258.
(25) Corani, A.; Pezzella, A.; Pascher, T.; Gustavsson, T.; Markovitsi, D.; Huijser, A.; d'Ischia, M.; Sundström, V. Excited-State Proton-Transfer Processes of DHICA Resolved: From Sub-Picoseconds to Nanoseconds. *J. Phys. Chem. Lett.* **2013**, *4*, 1383-1388.
(26) Huijser, A.; Pezzella, A.; Sundström, V. Functionality of Epidermal Melanin Pigments: Current Knowledge on UV-Dissipative Mechanisms and Research Perspectives. *Phys. Chem. Chem. Phys.* **2011**, *13*, 9119-9127.
(27) Gauden, M.; Pezzella, A.; Panzella, L.; Neves-Petersen, M. T.; Skovsen, E.; Petersen, S. B.; Mullen, K. M.; Napolitano, A.; d'Ischia, M.; Sundstrom, V. Role of Solvent, pH, and Molecular Size in Excited-State Deactivation of Key Eumelanin Building Blocks: Implications for Melanin Pigment Photostability. *J. Am. Chem. Soc.* **2008**, *130*, 17038-17043.
(28) Gauden, M.; Pezzella, A.; Panzella, L.; Napolitano, A.; d'Ischia, M.; Sundström, V. Ultrafast Excited State Dynamics of 5,6-dihydroxyindole, a Key Eumelanin Building Block: Nonradiative Decay Mechanism. *J. Phys. Chem. B* **2009**, *113*, 12575-12580.
(29) Premi, S.; Wallisch, S.; Mano, C. M.; Weiner, A. B.; Bacchiocchi, A.; Wakamatsu, K.; Bechara, E. J. H.; Halaban, R.; Douki, T.; Brash, D. E. Chemiexcitation of Melanin Derivatives Induces DNA Photoproducts Long After UV Exposure. *Science* **2015**, *347*, 842-847.
(30) Borovansky, J.; Riley, P. A. *Melanins and Melanosomes: Biosynthesis, Structure, Physiological and Pathological Functions*. John Wiley & Sons: Weinheim, Germany, 2011.
(31) Greenough, S. E.; Roberts, G. M.; Smith, N. A.; Horbury, M. D.; McKinlay, R. G.; Żurek, J. M.; Paterson, M. J.; Sadler, P. J.; Stavros, V. G. Ultrafast Photo-Induced Ligand Solvolysis of *cis*-$[Ru(bipyridine)_2(nicotinamide)_2]^{2+}$: Experimental and Theoretical Insight into its Photoactivation Mechanism. *Phys. Chem. Chem. Phys.* **2014**, *16*, 19141-19155.
(32) Greenough, S. E.; Horbury, M. D.; Thompson, J. O. F.; Roberts, G. M.; Karsili, T. N. V.; Marchetti, B.; Townsend, D.; Stavros, V. G. Solvent Induced Conformer Specific Photochemistry of Guaiacol. *Phys. Chem. Chem. Phys.* **2014**, *16*, 16187-16195
(33) Staniforth, M.; Young, J. D.; Cole, D. R.; Karsili, T. N. V.; Ashfold, M. N. R.; Stavros, V. G. Ultrafast Excited-State Dynamics of 2,4-Dimethylpyrrole. *J. Phys. Chem. A* **2014**, *118*, 10909-10918.
(34) Even, U.; Jortner, J.; Noy, D.; Lavie, N.; Cossart-Magos, C. Cooling of Large Molecules Below 1 K and He Clusters Formation. *The J. Chem. Phys.* **2000**, *112*, 8068-8071.
(35) Eppink, A. T. J. B.; Parker, D. H. Velocity Map Imaging of Ions and Electrons Using Electrostatic Lenses: Application in Photoelectron and Photofragment Ion Imaging of Molecular Oxygen. *Rev. Sci. Instrum.* **1997**, *68*, 3477-3484.
(36) Roberts, G. M.; Nixon, J. L.; Lecointre, J.; Wrede, E.; Verlet, J. R. R. Toward Real-Time Charged-Particle Image Reconstruction Using Polar Onion-Peeling. *Rev. Sci. Instrum.* **2009**, *80*, 053104.
(37) Roberts, G. M.; Chatterley, A. S.; Young, J. D.; Stavros, V. G. Direct Observation of Hydrogen Tunneling Dynamics in Photoexcited Phenol. *J. Phys. Chem. Lett.* **2012**, 348-352.
(38) Roberts, G. M.; Williams, C. A.; Yu, H.; Chatterley, A. S.; Young, J. D.; Ullrich, S.; Stavros, V. G. Probing Ultrafast Dynamics in Photoexcited Pyrrole: Timescales for $^1\pi\sigma^*$ Mediated H-atom Elimination. *Faraday Discuss.* **2013**, *163*, 95-116.
(39) Brede, O.; Kapoor, S.; Mukherjee, T.; Hermann, R.; Naumov, S. Diphenol Radical Cations and Semiquinone Radicals as Direct Products of the Free Electron Transfer from Catechol, Resorcinol and Hydroquinone to Parent Solvent Radical Cations. *Phys. Chem. Chem. Phys.* **2002**, *4*, 5096-5104.
(40) Land, E. J.; Porter, G. Primary Photochemical Processes in Aromatic Molecules Part 7. Spectra and Kinetics of Some Phenoxyl Derivatives. *T. Faraday Soc.* **1963**, *59*, 2016-2026.
(41) Owrutsky, J. C.; Raftery, D.; Hochstrasser, R. M. Vibrational Relaxation Dynamics in Solutions. *Annu. Rev. Phys. Chem.* **1994**, *45*, 519-555.
(42) Aßmann, J.; Kling, M.; Abel, B. Watching Photoinduced Chemistry and Molecular Energy Flow in Solution in Real Time. *Angew. Chem. Int. Edit.* **2003**, *42*, 2226-2246.
(43) Douhal, A.; Lahmani, F.; Zewail, A. H. Proton-Transfer Reaction Dynamics. *Chem. Phys.* **1996**, *207*, 477-498.
(44) Bent, D. V.; Hayon, E. Excited State Chemistry of Aromatic Amino Acids and Related Peptides. I. Tyrosine. *J. Am. Chem. Soc.* **1975**, *97*, 2599-2606.
(45) Karsili, T. N. V.; Wenge, A. M.; Harris, S. J.; Murdock, D.; Harvey, J. N.; Dixon, R. N.; Ashfold, M. N. R. O-H Bbond Fission in 4-Substituted Phenols: S_1 State Predissociation Viewed in a Hammett-like Framework. *Chem. Sci.* **2013**, *4*, 2434-2446.
(46) Pino, G. A.; Oldani, A. N.; Marceca, E.; Fujii, M.; Ishiuchi, S.-I.; Myazaki, M.; Broquier, M.; Dedonder, C.; Jouvet, C. Excited State Hydrogen Transfer Dynamics in Substituted Phenols and Their Complexes with Ammonia: $\pi\pi^*$ - $\pi\sigma^*$ Energy Gap Propensity and Ortho-Substitution Effect. *J. Chem. Phys.* **2010**, *133*, 124313

(47) Frisch, M. J.; Trucks G. W.; Schlegel, H. B.; Scuseria, G. E.; Robb, M. A.; Cheeseman, J. R.; Scalmani, G.; Barone, V.; Mennucci, B.; Petersson, G.A; et al. *Gaussian 09,* revision A.02; Gaussian, Inc. Wallingford, CT.
(48) Zhao, Y.; Schultz, N. E.; Truhlar, D. G. Design of Density Functionals by Combining the Method of Constraint Satisfaction with Parametrization for Thermochemistry, Thermochemical Kinetics, and Noncovalent Interactions. *J. Chem. Theory. Comput.* **2006**, *2*, 364-382.
(49) Yanai, T.; Tew, D. P.; Handy, N. C. A New Hybrid Exchange-Correlation Functional Using the Coulomb-Attenuating Method (CAM-B3LYP). *Chem. Phys. Lett.* **2004**, *393*, 51-57.
(50) Krishnan, R.; Binkley, J. S.; Seeger, R.; Pople, J. A. Self-Consistent Molecular Orbital Methods. XX. A Basis Set for Correlated Wave Functions. *J. Chem. Phys.* **1980**, *72*, 650-654.
(51) Varfolomeev, M. A.; Abaidullina, D. I.; Gainutdinova, A. Z.; Solomonov, B. N. FTIR Study of H-Bonds Cooperativity in Complexes of 1,2-dihydroxybenzene with Proton Acceptors in Aprotic Solvents: Influence of the Intramolecular Hydrogen Bond. *Spectrochim. Acta.* **2010**, *77*, 965-972.
(52) Navarrete, J. T. L.; Ramirez, F. J. A Study by Raman Spectroscopy and the Semiempirical AM1 Method on Several 1,2-dihydroxybenzene solutions. *Spectrochim. Acta.* **1993**, *49*, 1759-1767.
(53) Hermann, R.; Mahalaxmi, G. R.; Jochum, T.; Naumov, S.; Brede, O. Balance of the Deactivation Channels of the First Excited Singlet State of Phenols: Effect of Alkyl Substitution, Sterical Hindrance, and Solvent Polarity. *J. Phys. Chem. A* **2002**, *106*, 2379-2389.
(54) Machlin, L. J.; Bendich, A. Free Radical Tissue Damage: Protective Role of Antioxidant Nutrients. *FASEB J.* **1987**, *1*, 441-445.

Table of Contents (TOC) Image